Dalton Transactions

COMMUNICATION

Cite this: *Dalton Trans.*, 2017, **46**, 10197

Received 18th June 2017,
Accepted 3rd July 2017

DOI: 10.1039/c7dt02208e

rsc.li/dalton

High-performance adsorption and separation of anionic dyes in water using a chemically stable graphene-like metal–organic framework†

Jun-Jiao Li,[a] Chong-Chen Wang,*[a,b] Hui-fen Fu,[a] Jing-Rui Cui,[a] Peng Xu,[c] Jie Guo[a] and Jian-Rong Li*[d]

A highly stable graphene-like metal–organic framework (BUC-17) was prepared and used as an adsorbent to carry out the adsorption of anionic dyes from simulated wastewater, which exhibited excellent adsorption performance, particularly towards Congo red (CR) up to 4923.7 mg g^{-1} at room temperature. It was used to fix a SPE column to conduct rapid separation of anionic dyes from an organic dye matrix. A related mechanism was also proposed.

In the last two decades, remarkable progress has been achieved in the study of metal–organic frameworks (MOFs),[1] not only owing to their intriguing structures,[2] but also due to their interesting physical/chemical properties[3] and potential applications, such as in adsorption/separation,[4–10] catalysis,[11–13] photocatalysis,[14,15] luminescence,[16,17] magnetism,[18,19] electrical application,[20] sensing and recognition[21] and drug delivery.[22] Some MOFs have also been used to remove organic pollutants (including organic dyes), considering their striking characteristics of cavities with regular size and shape, well-defined channels, as well as excellent chemical and solvent stabilities.[23]

Recently, some MOFs were used to selectively adsorb and efficiently separate cationic or anionic dye molecules from their matrix due to the host–guest electronic interactions and/or guest–guest exchange interactions.[24–39] However, in most cases, the adsorption processes are time-consuming, and performed in non-aqueous solutions.[28,30–32] Without question, the practical application in this regard is mostly in aqueous solutions. Increasing attention is thus paid to how to efficiently separate organic dyes with similar sizes but different charges in aqueous solutions. On the other hand, it has been demonstrated that MOFs with exchangeable ions are desired to conduct high-performance adsorption and separation of organic pollutants.[40–42]

Cationic MOFs represent an appealing subclass, which are constructed from positively charged frameworks and weakly/non-coordinated counter anions lying in pores or interlayer spaces.[43] Considering that 1,3,5-tris(1-imidazolyl)benzene (tib, as illustrated in Fig. S1, ESI†), a rigid tridentate ligand, was once utilized as a versatile organic building unit to construct cationic coordination architectures with interesting structures, topologies, and properties,[44–46] in this study, we selected this ligand to construct a new two-dimensional (2D) MOF, $[Co_3(tib)_2(H_2O)_{12}](SO_4)_3$ (**BUC-17**) under hydrothermal conditions. The X-ray single-crystal diffraction structural analysis (Tables S1 and S2, ESI†) reveals that the octahedral geometry of the Co(II) atom in **BUC-17** (Fig. 1b) is completed by two nitrogen atoms from two different tib ligands, occupying the two axial positions, and four oxygen atoms from four coordinated water molecules, which lie in the four sites of the equatorial plane. Six Co(II) atoms are connected by six tib ligands to form a graphene-like hexagonal pore subunit with an aperture size of *ca.* 2.36 nm (Fig. 1a and c). These subunits

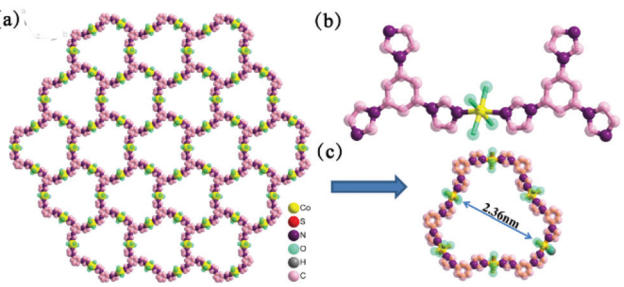

Fig. 1 (a) The 2D framework structure of **BUC-17**. (b) A symmetric unit of **BUC-17** and coordination environments of Co atoms. H atoms are omitted for clarity. (c) The hexagonal hole in **BUC-17**.

[a]*Beijing Key Laboratory of Functional Materials for Building Structure and Environment Remediation, Beijing University of Civil Engineering and Architecture, Beijing, 100044, China. E-mail: chongchenwang@126.com*
[b]*Beijing Advanced Innovation Centre for Future Urban Design, Beijing University of Civil Engineering and Architecture, Beijing, 100044, China*
[c]*CAS Key Laboratory of Standardization and Measurement for Nanotechnology, National Centre for Nanoscience and Technology, Beijing, 100190, P. R China*
[d]*Department of Chemistry and Chemical Engineering, College of Environmental and Energy Engineering, Beijing University of Technology, Beijing 100022, China. E-mail: jianrongli@bjut.edu.cn*

†Electronic supplementary information (ESI) available. CCDC 1482297. For ESI and crystallographic data in CIF or other electronic format see DOI: 10.1039/c7dt02208e

are arrayed to form final cationic 2D $[Co_3(tib)_2(H_2O)_{12}]^{n+}$ sheets, which are further linked to form a 3D supramolecular framework through abundant hydrogen-bonding interactions (Fig. S3 and Table S3 in the ESI†). The uncoordinated sulfate (SO_4^{2-}) anions thus act as discrete counter-ions to compensate the cationic charges of the $[Co_3(tib)_2(H_2O)_{12}]^{n+}$ layer.

To investigate the performance of **BUC-17** toward removing organic pollutants, adsorption experiments were performed in a batch system, in which some typical organic dyes like congo red (**CR**), mordant blue 13 (**MB13**), methylene blue (**MB**), and sudan I (**SI**) (Fig. S2, ESI†) were selected as targeted models. The adsorption activities of **BUC-17** toward anionic **CR** were described in detail, while the adsorption towards **MB13**, **MB**, and **SI** is described in the ESI.† As illustrated in Fig. S4a (ESI†), 99.1% **CR** was removed *via* **BUC-17** in 3.0 min, implying that **BUC-17** could conduct rapid and high-performance adsorption/capture of **CR**. The adsorption capacity of **BUC-17** towards **CR** was determined to be 4923.7 mg g^{-1} at room temperature, much higher than most of the adsorbents reported previously (as listed in Table S4, ESI†).

BUC-17 was stable under air and in water, also insoluble in water and common organic solvents, including ethanol, methylbenzene, chloroform, ether, DMSO and DMF, which was confirmed by powder X-ray diffraction. It was found that the experimental patterns matched well with those patterns simulated from the single-crystal X-ray diffraction data, indicating that **BUC-17** was in high purity (Fig. 2a). The PXRD patterns of **BUC-17** after adsorbing **CR** and being immersed in water solution up to 72 h were also completely consistent with those of the as-prepared **BUC-17**, implying its excellent stability in water. Moreover, the adsorption of **CR** onto **BUC-17** was further affirmed by TGA, as shown in Fig. 2b, in which there

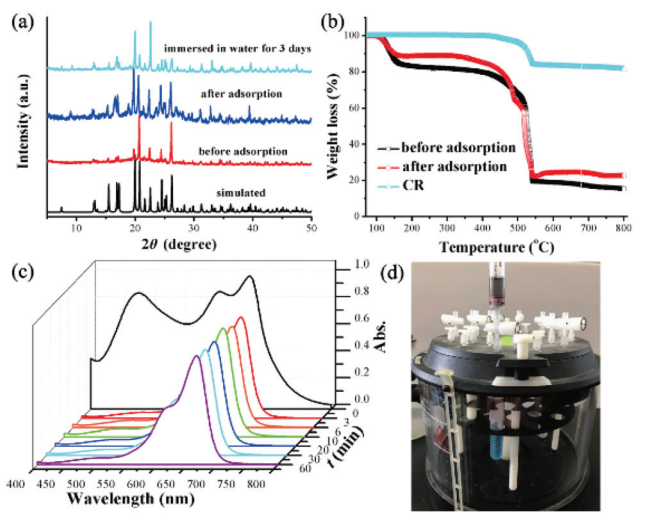

Fig. 2 (a) Comparison of PXRD patterns of the simulated one from single crystal data, **BUC-17** before and after adsorbing **CR**, as well as being immersed in water for 3 d. (b) TGA curve of the as-synthesized **BUC-17**, **CR** dye and **BUC-17** after adsorbing **CR**. (c) UV-Vis spectral changes of the dye mixtures of **CR** and **MB** in a batch system. (d) The picture of the SPE setup.

was a new weight loss in the TGA curve of **CR@BUC-17**. Also, the framework of **BUC-17** was stable under 400 °C as shown in Fig. 2b. The adsorption of **CR** onto **BUC-17** was also affirmed by FTIR, and XPS, as illustrated in Fig. S5, ESI.†

To clarify the detailed adsorption behavior of **BUC-17** towards **CR**, the adsorption kinetics, isotherm models and related thermodynamic parameters are calculated. Adsorption kinetics like the pseudo-first-order model and pseudo-second-order model are usually applied to predict the controlling mechanism of adsorptions.[47] The calculated k_1 and k_2 values and the corresponding linear regression correlation coefficient (R^2) values of the above-stated models are shown in Table S5 (ESI†). The obtained R^2 values for the pseudo-second-order model are above 0.99 at different initial **CR** concentrations. The good agreement with the pseudo-second-order model was also confirmed by similar values of calculated q_e and the experimental ones, as listed in Table S5 (ESI†), demonstrating that the rate-limiting step might be chemisorption involving valence forces through sharing or exchange of electrons.[48,49]

Also, adsorption isotherms are important to describe how the adsorbate molecules interact with the adsorbent surface.[50] Three isotherm models, Langmuir, Freundlich, and Dubinin-Radushkevich (D-R), were herein utilized to elaborate the behavior of **CR** adsorption onto **BUC-17**. Related experiments were conducted at 288, 293, 298, 303, and 308 K, respectively. As shown in Table S6 (ESI†), the high coefficients R^2 (ranging from 0.970 to 0.999) of Langmuir equations implied that the adsorption of **CR** onto **BUC-17** fitted well with the Langmuir model. The q_{max} values obtained from the Langmuir model increased with the temperature, indicating that the adsorption as an endothermic process was favorable at high temperatures.

The standard free energy ΔG^0, enthalpy ΔH^0, and entropy ΔS^0 were calculated based on the data obtained from the Langmuir adsorption isotherm (Table S7 in the ESI†) to clarify the thermodynamic functions and the effects of the temperature on the process of **CR** adsorption onto **BUC-17**. The negative ΔG^0 values ranging from −23.80 to −32.47 kJ mol^{-1} with the temperature increasing from 288 to 308 K confirmed that the adsorption of **CR** onto **BUC-17** was feasible and spontaneous thermodynamically,[51] thus the adsorption process became more favorable at high temperatures.[52] The positive value of ΔS^0 (407 J mol^{-1} K^{-1}) indicated the randomness increased at the solid/solution interface during the adsorption process.[53] The positive values of ΔH^0 (92.62 kJ mol^{-1}) demonstrated that the adsorption process was endothermic,[54] which was similar to the adsorption of **CR** onto **AC**.[55]

Besides **CR**, **BUC-17** also exhibited excellent adsorption performance toward anionic **MB13** (Fig. S4b in the ESI†). But, it was inhospitable to cationic **MB** and neutral **SI** as stated in the ESI.† The colors of **MB** and **SI** solutions remained unchanged after more than 120 min of contact with **BUC-17**, as shown in Fig. S6 of the ESI.† Based on the preferential uptake of **BUC-17** towards anionic dyes and inert action to cationic/neutral dyes, a series of experiments were designed to test its potential separation ability for **CR** (100 mg L^{-1})/**MB** (20 mg L^{-1}) and **MB13**

(20 mg L^{-1})/**MB** (20 mg L^{-1}) matrixes, respectively (detailed experimental description is provided in the ESI†).

Solid phase extraction (SPE) was also adopted to conduct the **CR** (100 mg L^{-1})/**MB** (20 mg L^{-1}) matrix separation, in which the Agilent Bond Elut C18 in a commercially available SPE column was replaced with 1.0 g **BUC-17** with a particle size of about 0.08 mm. The **CR**/**MB** matrix (C_{CR} = 100 mg L^{-1} and C_{MB} = 20 mg L^{-1}) was pumped through the SPE column *via* automatic vacuum with a flow rate of 5 mL min^{-1} (Fig. 2d, and Video 1, ESI†). It was found that the **MB**, inert to **BUC-17**, passed through the SPE column completely and quickly, whereas the **CR** was retained in **BUC-17**, indicating that **BUC-17** could rapidly and efficiently separate **CR** and **MB** from their mixture.

The BET surface area of **BUC-17** is 2.39 m^2 g^{-1}, demonstrating that its high-performance towards anionic dyes might not be attributed to its porosity,[30] while **BUC-17** preferring to capture anionic dyes like **CR** and **MB13** can be partly attributed to its positive pore surface charge, as confirmed by the tested zeta potential ranging from 14.0 to 24.9 mV at pH 4.0–10.0. As stated above, the pore size of **BUC-17** is *ca.* 2.36 nm, smaller than the molecule sizes of anionic **CR** (2.61 × 0.86 × 0.39 nm) and bigger than the size of **MB13** (1.56 × 0.86 × 0.62 nm), respectively. But, its adsorption performances towards **CR** (q_{max} being 4923.7 mg g^{-1}) and **MB13** (q_{max} being 850.5 mg g^{-1}) are different, indicating that the molecule size might not contribute to the ultra-high uptake amount of **CR**. In the **BUC-17** structure, the uncoordinated SO_4^{2-} anions are supposed to be exchanged with the anionic dyes during adsorption,[30] which was confirmed by its adsorption performance towards **CR** (100 mg L^{-1}) in saturated aqueous Na_2SO_4 solution and in pure aqueous solution. These results revealed that the presence of SO_4^{2-} obviously inhibited the **CR** adsorption onto **BUC-17**, as evidenced by the adsorption efficiency decrease from 95.4% (in pure aqueous solution) to 76.8% (saturated Na_2SO_4 aqueous solution) within 60 min, as illustrated in Fig. 3(a). In general, PO_4^{3-} is deemed as a much stronger competitor than SO_4^{2-} in ion-exchange adsorption systems.[56,57] The anionic **CR** could be desorbed from **CR@BUC-17** in Na_3PO_4 solution *via* the exchange between anionic **CR** and PO_4^{3-} (as shown in Fig. 3b), in which the desorbed **CR** amount is 1692.0 mg g^{-1}, *ca.* 1/3 of **BUC-17**'s maximum adsorption capacity of 4923.7 mg g^{-1}, implying that ion exchange might not be the only mechanism resulting in the ultra-high adsorption performance of **BUC-17**.[58,59] It is worth noting that it was difficult to desorb **CR** from **CR@BUC-17** in common solvents like deionized water and ethanol, as shown in Fig. 3(b).

The presence of the coordinated water molecules in **BUC-17** and amino/sulfonic groups in **CR** might contribute to form abundant hydrogen-bonding interactions, which could favour **CR** adsorbtion.[60,61] In FTIR spectra, a noticeable blue shift could be observed, which could be assigned to the –OH stretching vibration band shifting from 3360 cm^{-1} of **BUC-17** to 3419 cm^{-1} after **CR@BUC-17** (Fig. S5a, ESI†). And, a new absorption band at 1426 cm^{-1} ($-NH_2$ bending vibration) of **CR@BUC-17** appeared, which could be ascribed to the hydrogen-bonding interaction between the hydroxyl ion of coordinated H_2O in **BUC-17** and amino groups of the **CR**[62–64] (Fig. S3a, ESI†). The XPS spectra indicate that the adsorption of **CR** by **BUC-17** led to a shift of the O 1s peak to higher energy, from 530.85 eV to 531.16 eV, which could be ascribed to the hydrogen bonding interaction between the hydroxyl ion of coordinated H_2O of **BUC-17** and anionic sulfonic groups of the **CR** dye.[62] The sulfonic groups of **CR** might also facilitate the formation of hydrogen-bonding interactions with the coordinated H_2O molecules after adsorption. The hydrogen bonding hypothesis could also explain the very different adsorption capacities between **CR** and **MB13**, in which the $-NH_2$ groups in **CR** facilitate to form hydrogen-bonding interactions, while there were no effective hydrogen-bonding functional groups in **MB13** due to the absence of $-NH_2$ groups. Furthermore, the π–π stacking interactions between the aromatic rings of **CR** and the imidazole ring of **BUC-17** might contribute to its excellent adsorption performance towards **CR**.[65,66] In addition, the hexagonal pore size of *ca.* 2.36 nm in **BUC-17** fell into the scope of the mesopore, which was also beneficial for promoting the adsorption activity due to the mesopore effect.[67] In all, as shown in Fig. 4, the possible mechanisms involved in the adsorption process could clarify its excellent adsorption performance towards **CR** and efficient separation of **CR** from the **CR**/**MB** mixture.

In conclusion, a water-stable MOF **BUC-17** was successfully synthesized, which exhibited ultra-high adsorption capacity

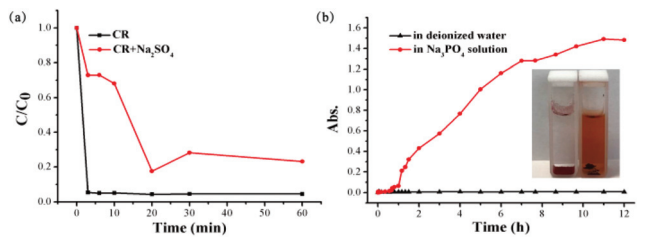

Fig. 3 (a) Adsorption of **CR** in deionized water and in saturated Na_2SO_4 solution with **BUC-17**. (b) The **CR** release from **CR@BUC-17** in deionized water and in saturated Na_3PO_4 solution.

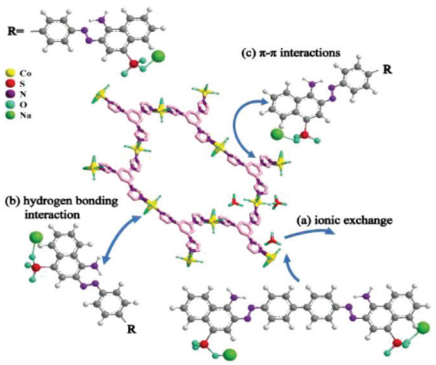

Fig. 4 Proposed interaction mechanism between **CR** and **BUC-17**.

towards **CR** (4923.7 mg **CR** per gram of **BUC-17**). The adsorption process followed a pseudo-second-order kinetic model and fitted well with the Langmuir isotherm. The possible mechanisms were proposed, including the positive surface charge, ion-exchange, hydrogen-bonding interactions, and π–π stacking interactions along with the effect of mesopores. **BUC-17** can achieve such advantages as time-saving, water stability, and ultra-high adsorption capacity. Furthermore, **BUC-17** was used to prepare a SPE column to efficiently separate different organic dyes from their mixture in water. Considering the ultra-high adsorption performance and efficient separation ability of **BUC-17**, it is believed that more potential applications can be developed in real environment samples.

The authors acknowledge financial support from the National Natural Science Foundation of China (51578034 and 21576006), the Beijing Natural Science Foundation & Scientific Research Key Program of Beijing Municipal Commission of Education (KZ201410016018), the Beijing Talent Project (2016023) and the BUCEA Post Graduate Innovation Project (PG2017012).

Notes and references

1 C.-C. Wang and Y.-S. Ho, *Scientometrics*, 2016, **109**, 481–513.
2 L. L. Lv, J. Yang, H. M. Zhang, Y. Y. Liu and J. F. Ma, *Inorg. Chem.*, 2015, **54**, 1744–1755.
3 Z. Su, J. Xu, F. Jian, D.-J. Liu, Q. Chu, M.-S. Chen, S.-S. Chen, G.-X. Liu, X.-F. Wang and W.-Y. Sun, *Cryst. Growth Des.*, 2009, **9**, 2801–2811.
4 P.-Y. Du, H. Li, X. Fu, W. Gu and X. Liu, *Dalton Trans.*, 2015, **44**, 13752–13759.
5 H. Furukawa, N. Ko, Y. B. Go, N. Aratani, S. B. Choi, E. Choi, A. O. Yazaydin, R. Q. Snurr, M. O'Keeffe, J. Kim and O. M. Yaghi, *Science*, 2010, **329**, 424–428.
6 R. P. Ojha, P. A. Lemieux, P. K. Dixon, A. J. Liu and D. J. Durian, *Nature*, 2004, **427**, 521–523.
7 B. Wang, X. L. Lv, D. Feng, L. H. Xie, J. Zhang, M. Li, Y. Xie, J. R. Li and H. C. Zhou, *J. Am. Chem. Soc.*, 2016, **138**, 6204–6216.
8 Y. Li, C. X. Yang and X. P. Yan, *Chem. Commun.*, 2017, **53**, 2511–2514.
9 P. Nugent, Y. Belmabkhout, S. D. Burd, A. J. Cairns, R. Luebke, K. Forrest, T. Pham, S. Ma, B. Space, L. Wojtas, M. Eddaoudi and M. J. Zaworotko, *Nature*, 2013, **495**, 80–84.
10 Q. Gao, J. Xu, D. Cao, Z. Chang and X. H. Bu, *Angew. Chem., Int. Ed.*, 2016, **55**, 15027–15030.
11 L. Cao, Z. Lin, F. Peng, W. Wang, R. Huang, C. Wang, J. Yan, J. Liang, Z. Zhang and T. Zhang, *Angew. Chem., Int. Ed.*, 2016, **55**, 4962–4966.
12 S. Yuan, L. Zou, H. Li, Y. P. Chen, J. Qin, Q. Zhang, W. Lu, M. B. Hall and H. C. Zhou, *Angew. Chem., Int. Ed.*, 2016, **55**, 10776–10780.
13 Y. K. Hwang, D.-Y. Hong, J.-S. Chang, S. H. Jhung, Y.-K. Seo, J. Kim, A. Vimont, M. Daturi, C. Serre and G. Férey, *Angew. Chem., Int. Ed.*, 2008, **120**, 4212–4216.
14 C.-C. Wang, X.-D. Du, J. Li, X.-X. Guo, P. Wang and J. Zhang, *Appl. Catal., B*, 2016, **193**, 198–216.
15 K. M. Choi, D. Kim, B. Rungtaweevoranit, C. A. Trickett, J. T. Barmanbek, A. S. Alshammari, P. Yang and O. M. Yaghi, *J. Am. Chem. Soc.*, 2017, **139**, 356–362.
16 Y. Guo, X. Feng, T. Han, S. Wang, Z. Lin, Y. Dong and B. Wang, *J. Am. Chem. Soc.*, 2014, **136**, 15485–15488.
17 Z. Ye, X. An, B. Song, W. Zhang, Z. Dai and J. Yuan, *Dalton Trans.*, 2014, **43**, 13055–13060.
18 M. Kurmoo, *Chem. Soc. Rev.*, 2009, **38**, 1353–1379.
19 E. Coronado and G. Minguez Espallargas, *Chem. Soc. Rev.*, 2013, **42**, 1525–1539.
20 W. Zhang and R. G. Xiong, *Chem. Rev.*, 2011, **112**, 1163–1195.
21 H. Wang, J. Xu, D. S. Zhang, Q. Chen, R. M. Wen, Z. Chang and X. H. Bu, *Angew. Chem., Int. Ed.*, 2015, **54**, 5966–5970.
22 Y.-Q. Chen, G.-R. Li, Z. Chang, Y.-K. Qu, Y.-H. Zhang and X.-H. Bu, *Chem. Sci.*, 2013, **4**, 3678–3682.
23 E. Haque, J. W. Jun and S. H. Jhung, *J. Hazard. Mater.*, 2011, **185**, 507–511.
24 A. X. Yan, S. Yao, Y. G. Li, Z. M. Zhang, Y. Lu, W. L. Chen and E. B. Wang, *Chem. – Eur. J.*, 2014, **20**, 6927–6933.
25 Z. Zhu, Y.-L. Bai, L. Zhang, D. Sun, J. Fang and S. Zhu, *Chem. Commun.*, 2014, **50**, 14674–14677.
26 D.-m. Chen, W. Shi and P. Cheng, *Chem. Commun.*, 2015, **51**, 370–372.
27 Y.-C. He, J. Yang, W.-Q. Kan, H.-M. Zhang, Y.-Y. Liu and J.-F. Ma, *J. Mater. Chem. A*, 2015, **3**, 1675–1681.
28 X.-L. Lv, M. Tong, H. Huang, B. Wang, L. Gan, Q. Yang, C. Zhong and J.-R. Li, *J. Solid State Chem.*, 2015, **223**, 104–108.
29 Q. Chen, Q. He, M. Lv, Y. Xu, H. Yang, X. Liu and F. Wei, *Appl. Surf. Sci.*, 2015, **327**, 77–85.
30 L. Xiao, Y. Xiong, S. Tian, C. He, Q. Su and Z. Wen, *Chem. Eng. J.*, 2015, **265**, 157–163.
31 H.-N. Wang, F.-H. Liu, X.-L. Wang, K.-Z. Shao and Z.-M. Su, *J. Mater. Chem. A*, 2013, **1**, 13060–13063.
32 Y.-C. He, J. Yang, W.-Q. Kan, H.-M. Zhang, Y.-Y. Liu and J.-F. Ma, *J. Mater. Chem. A*, 2015, **3**, 1675–1681.
33 Y. Fan, H.-J. Liu, Y. Zhang and Y. Chen, *J. Hazard. Mater.*, 2015, **283**, 321–328.
34 F.-Y. Yi, W. Zhu, S. Dang, J.-P. Li, D. Wu, Y.-h. Li and Z.-M. Sun, *Chem. Commun.*, 2015, **51**, 3336–3339.
35 Z. Hasan and S. H. Jhung, *J. Hazard. Mater.*, 2015, **283**, 329–339.
36 J. Huo, J. Aguilera-Sigalat, S. El-Hankari and D. Bradshaw, *Chem. Sci.*, 2015, **6**, 1938–1943.
37 Y.-X. Tan, Y.-P. He, M. Wang and J. Zhang, *RSC Adv.*, 2014, **4**, 1480–1483.
38 S. Kumar, G. Verma, W.-Y. Gao, Z. Niu, L. Wojtas and S. Ma, *Eur. J. Inorg. Chem.*, 2016, **2016**, 4373–4377.

39 B. Li, Y. Zhang, D. Ma, Z. Xing, T. Ma, Z. Shi, X. Ji and S. Ma, *Chem. Sci.*, 2016, **7**, 2138–2144.
40 I. R. Colinas, K. K. Inglis, F. Blanc and S. R. J. Oliver, *Dalton Trans.*, 2017, **46**, 5320–5325.
41 J. Li, H. R. Fu, J. Zhang, L. S. Zheng and J. Tao, *Inorg. Chem.*, 2015, **54**, 3093–3095.
42 A. Planchais, S. Devautour-Vinot, S. Giret, F. Salles, P. Trens, A. Fateeva, T. Devic, P. Yot, C. Serre, N. Ramsahye and G. Maurin, *J. Phys. Chem. C*, 2013, **117**, 19393–19401.
43 X. Zhao, C. Mao, K. T. Luong, Q. Lin, Q. G. Zhai, P. Feng and X. Bu, *Angew. Chem., Int. Ed.*, 2016, **128**, 2818–2822.
44 Z. Su, Z.-B. Wang and W.-Y. Sun, *Inorg. Chem.*, 2010, **13**, 1278–1280.
45 L. Li, J. Fan, T.-A. Okamura, Y.-Z. Li, W.-Y. Sun and N. Ueyama, *Supramol. Chem.*, 2004, **16**, 361–370.
46 J. Fan, W. Y. Sun, T. A. Okamura, W. X. Tang and N. Ueyama, *Inorg. Chem.*, 2003, **42**, 3168–3175.
47 Y. S. Ho, *J. Hazard. Mater.*, 2006, **37**, 681–689.
48 F. A. Pavan, S. L. P. Dias, E. C. Lima and E. V. Benvenutti, *Dyes Pigm.*, 2008, **76**, 64–69.
49 V. Vimonses, S. Lei, B. Jin, C. W. K. Chow and C. Saint, *Chem. Eng. J.*, 2009, **148**, 354–364.
50 E. Lorencgrabowska and G. Gryglewicz, *Dyes Pigm.*, 2007, **74**, 34–40.
51 A. Sari, M. Tuzen, D. Citak and M. Soylak, *J. Hazard. Mater.*, 2007, **149**, 283–291.
52 A. B. Zaki, M. Y. El-Sheikh, J. Evans and S. A. El-Safty, *J. Colloid Interface Sci.*, 2000, **221**, 58–63.
53 A. Ozcan, A. Ozcan, S. Tunali, T. Akar and I. Kiran, *J. Hazard. Mater.*, 2005, **124**, 200–208.
54 A. Mittal, D. Jhare and J. Mittal, *J. Mol. Liq.*, 2013, **179**, 133–140.
55 C. Namasivayam and D. Kavitha, *Dyes Pigm.*, 2002, **54**, 47–58.
56 M. Sui, L. Sheng, K. Lu and F. Tian, *Appl. Catal., B*, 2010, **96**, 94–100.
57 J. S. Geelhoed, T. Hiemstra and W. H. V. Riemsdijk, *Geochim. Cosmochim. Acta*, 1997, **61**, 2389–2396.
58 J. Jia, F. Sun, T. Borjigin, H. Ren, T. Zhang, Z. Bian, L. Gao and G. Zhu, *Chem. Commun.*, 2012, **48**, 6010–6012.
59 C. Y. Sun, X. L. Wang, C. Qin, J. L. Jin, Z. M. Su, P. Huang and K. Z. Shao, *Chemistry*, 2013, **19**, 3639–3645.
60 I. Ahmed and S. H. Jhung, *Chem. Eng. J.*, 2016, **310**, 197–215.
61 V. Jabbari, J. M. Veleta, M. Zarei-Chaleshtori, J. Gardea-Torresdey and D. Villagrán, *Chem. Eng. J.*, 2016, **304**, 774–783.
62 H. Hou, R. Zhou, P. Wu and L. Wu, *Chem. Eng. J.*, 2012, **211–212**, 336–342.
63 J. Shu, Z. Wang, Y. Huang, N. Huang, C. Ren and W. Zhang, *J. Alloys Compd.*, 2015, **633**, 338–346.
64 S.-X. Teng, S.-G. Wang, X.-W. Liu, W.-X. Gong, X.-F. Sun, J.-J. Cui and B.-Y. Gao, *Colloids Surf., A*, 2009, **340**, 86–92.
65 M. S. Tehrani and R. Zare-Dorabei, *Spectrochim. Acta, Part A*, 2016, **160**, 8–18.
66 A. Ayati, M. N. Shahrak, B. Tanhaei and M. Sillanpaa, *Chemosphere*, 2016, **160**, 30–44.
67 X.-X. Huang, L.-G. Qiu, W. Zhang, Y.-P. Yuan, X. Jiang, A.-J. Xie, Y.-H. Shen and J.-F. Zhu, *CrystEngComm*, 2012, **14**, 1613–1617.